Master's Thesis of Engineering

# Designed Functional Molecule for High Stable and Efficient Perovskite Solar Cells

## 고안정성/고효율 페로브스카이트 태양전지를 위한 분자 구조 설계

August 2019

Graduate School of Engineering
Seoul National University
Mechanical Engineering

Piao Chengcheng

# Designed Functional Molecule for High Stable and Efficient Perovskite Solar Cells

Advising Professor: Choi, Mansoo

Submitting a master's thesis of Public Administration

April 2019

Graduate School of Engineering
Seoul National University
Mechanical Engineering

Piao Chengcheng

Confirming the master's thesis written by
Piao Chengcheng
June 2019

Chair Lee, Junghoon (Seal)
Vice Chair Choi, Mansoo (Seal)
Examiner Shin, Yongdae (Seal)

# Abstract

## Designed Functional Molecule for High Stable and Efficient Perovskite Solar Cells

Piao Chengcheng

School of Mechanical and Aerospace Engineering

The Graduate School

Seoul National University

Perovskite solar cells have showed outstanding advantage as a clean energy because of their rapid development of power conversion efficiency (PCE) and low cost. However, the stability problem still limits their practical applications and commercialization. To overcome the degradation issue, here we designed a novel molecule to achieve the post-modification of the interface of perovskite layer. With the designed passivation molecule, the halide vacancies at interface has been efficiently decreased and the performance of devices gets a distinct promotion. When embodying the passivation layer, the photovoltaic cells exhibit an enhanced PCE of 20.03. In addition, when compared to pristine perovskite solar cell, the stability greatly improved, which retain 60% of the initial PCE for 800 hours at ambient environment.

**Keyword :** Perovskite solar cells, Passivation molecule, Stability

**Student Number :** 2017-24291

# Table of Contents

# List of Figures

# Chapter 1. Introduction

## 1.1. Study background

As the rapid development of science and technology, the demand for energy is increasing contemporarily. Although fossil resources are still the most important source at present, the limitation of reserves is gradually depleted. At the same time, the pollutants produced by its combustion have caused great harms to the environment and humans. Especially, the formation of haze worldwide has become an environment issue that needs to be addressed. Therefore, seeking renewable green energy has become a serious and urgent task.

### 1.1.1. Overview of solar cells

Nowadays, clean energy such as solar energy, wind energy, geothermal energy and ocean energy have achieved rapid development around the world. [1−3] Along these fields, solar energy has received the highest attention due to its characteristics of pollution−free, high−energy storage and wide range. Based on this, the utilization of solar energy has been vigorously promoted and developed, which mainly includes two aspects: light energy converts to thermal energy and electrical energy. The light−to−heat conversion is carried out by absorbing and reflecting the energy generated by the solar radiation, so that the generated heat energy can be used in different fields, commonly, such as solar water heater, solar combustion stove, solar greenhouse, etc. Photoelectric conversion is a conversion from solar energy into electrical energy through the photovoltaic effect. Photovoltaic is the effect that when semiconductor material absorbs photons, the carrier concentration gradient formed which lead to a formation of photocurrent. Photovoltaic effect was first discovered by French AE Becquerel in 1839, now mainly used in solar cells. However, solar cells have experienced a century of development after invention, efficiency was

still less than 1%, and humans still face this thorny problem. For a deeper understanding of solar cells and a broader study of semiconductor materials, Bell Labs in the United States developed a P-N junction solar cell based on silicon semiconductor with the efficiency up to 6.0% in 1954, officially opening up a flourish of solar cells. [4]

At present, the technological level of silicon semiconductor-based solar cells is approaching maturity, and the photoelectric conversion efficiency has reached 26.6%, making a historic breakthrough and has already begun using in outer space. [5] At the same time, the development of multi-junction cells is another way to further improve efficiency. However, due to the high cost of silicon, which restricts its commercial development, people have gradually developed second-generation solar cells based on compound semiconductor films (such as GaAs, CdTe, CIGS, etc.), taking into account the advantages of high efficiency and stability, it has been widely favored in the commercial field. [6] Nevertheless, the large-scale application of such batteries restricted by the processing technology, the scarcity of rare materials and the pollution of energy consumption problems.

To reduce production costs and optimize processing technology, the third generation of solar cells came into being, mainly including: dye-sensitized solar cells, organic solar cells and quantum dot sensitized solar cells. [7-9] Such batteries can be prepared by a solution method, which is simple and has low material cost. So it is advantageous to mass production. Nonetheless, due to the low carrier migration rate, the efficiency of such solar cells is still less than 16%, which is difficult to compete with high-efficiency silicon-based and compound semiconductor thin film solar cells, these solar cells has reached a bottleneck for its development. [5]

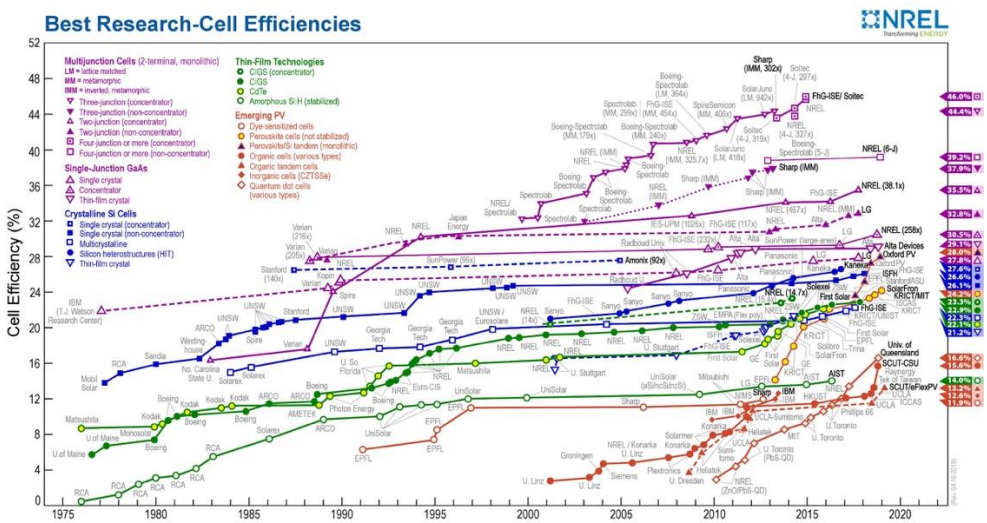

Figure 1-1 Best Research-Cell Efficiency Chart of 2019 [5]

In order to further meet the needs of the photovoltaic commercial market, balancing the efficiency and processing cost of photovoltaic devices while optimizing has become the most important issue, and the core of breakthrough is to choose appropriate semiconductor materials. Faced with the choice of tens of thousands of materials, organic-inorganic hybrid perovskite (perovskite) materials are rapidly emerging at low cost, simple process and excellent photoelectric performance. From Figure 1-1, we can find that after only 10 years of development of perovskite solar cells, now the efficiency has been comparable with other types of solar cells, which spectacularly reached to 24.2%. [5]

## 1.1.2. Working mechanism of solar cells

The structure of a conventional solar cell is as shown in Figure 1-2. Depending on the type of doping, semiconductor materials are generally classified into electron type (N type) and hole type (P type). When two opposite doping types of semiconductor are in contact, a space-charge region (PN junction) is generated at the interface. The basic working principle of solar cells is based on the photovoltaic effect of semiconductors. Under the solar radiation, a trapped electron-hole pair (excitons) is formed at the PN junction.

When the exciton binding energy is small, electrons and hole would diffuse freely from high concentration to low concentration, forming a built-in electric field, which is captured at the electrodes at both ends to generate current. The essence of the whole process is to convert photon energy into electrical energy. [10] In addition, when the exciton binding energy is large, electrons and holes have a certain probability of recombination. The radiation transition also occurs accompanied by the release of photons, so that the photon absorption and utilization ratio are greatly reduced, which is disadvantageous to the carrier transport inside of the device. [10]

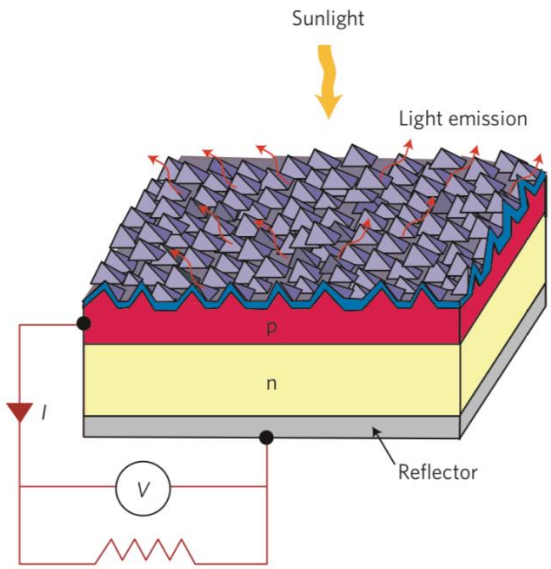


Figure 1-2 Working mechanism of solar cells [10]

### 1.1.3. Characteristic parameter of solar cells

To unify the test condition of solar cells in laboratory and reduce the influence of solar radiation in different latitudes and regions, International Electrotechnical Commission TC82 stipulated the standard test conditions as follows: AM 1.5G is the standard irradiance of sunlight, corresponding to the elevation angle of view of 41.8° and the spectral intensity is 1000W/$m^2$.

Generally, characterizing the performance of a solar cell is to apply a bias voltage to the device. While under AM1.5 standard

sunlight, the device is driven to work externally as the bias voltage changes, and the corresponding current−voltage is obtained. There are four important parameters for evaluating solar cell performance include: short circuit current density (Jsc), open circuit voltage (Voc), fill factor (FF), and photoelectric conversion efficiency (PCE).

1) Short circuit current density (Jsc)

Under the AM1.5 standard sunlight, the solar cell is at zero external voltage, that is, the maximum current density of the internal output of the battery at the short−circuit condition, and the corresponding value is the intersection of the J−V curve and the ordinate. The formation of the short−circuit current has a certain difference between the work function of the two side of the device. When the device is short−circuited, the built−in electric field inside the device drives the separation of the photo−generated carriers, thereby forms a short−circuit current. When the device is in actual operation, the choice of semiconductor material, the difference in battery working area and internal device structure will affect the value of Jsc: the narrower the forbidden band width of semiconductor material, the wider the spectrum of solar energy that can be captured, corresponding a higher density of carrier and a higher Jsc. With a smaller working area of the battery, the area under light irradiation would be more uniform, so that the defect state inside the battery gets smaller, Jsc would increase. In addition, when the energy level inside the device and the contact at the interface is arranged more reasonable, the probability of photo−generated carrier separation would increase, and the energy loss of the radiation transition would decrease, which is beneficial of improving Jsc.

2) Open circuit voltage (Voc)

Under AM1.5 standard sunlight, the solar cell is at zero current output, that is, the maximum voltage provided inside the battery at the open state, and the corresponding value is the intersection of the J−V curve and the abscissa. The formation of the open circuit voltage is related to the strength of the built−in electric field of the device under illumination. When the device is in an open circuit, photo generated carriers accumulate at the edge of the depletion region to

cancel the built-in electric field, thereby forming an open circuit voltage. Similarly, Voc is influenced by the choice of semiconductor materials, the difference in electrode work function and the distribution of internal interfaces: the larger the forbidden band width of semiconductor materials, the stronger the built-in electric field is, which contributes to an increase of Voc. The more difference in electrode work function, closer to the potential difference of the pn junction, the higher the Voc will be. In addition, when the internal interface distribution is mush uniform, the series resistance of the internal resistance of the battery will decrease, and Voc will increase simultaneously.

3) Fill factor (FF)

FF, characterizing the maximum output power of a solar cell, is formulated as

$$FF=\frac{Jmp*Vmp}{Jsc*Voc} \quad , \qquad (1-1)$$

where Jmp is the current density corresponding to the maximum output power Pmax at the J-V curve; Vmp is the voltage corresponding to Pmax at the J-V curve. FF essentially characterizes the ratio of electron-hole pairs and photogenerated carriers that generate photocurrent in a solar cell. A larger FF represent a lower exciton separation rate and recombination rate, and also a higher photon utilization.

4) Photoelectric conversion efficiency (PCE)

PCE, represents the ratio of the solar cell's unit area to the incident light energy converted into electrical energy, is the ratio of the maximum output power Pmax of the solar cell to the incident power of the solar light.

$$PCE=\frac{Pmax}{Pin}=\frac{FF*Jsc*Voc}{Pin}, \qquad (1-2)$$

In the formula, Pin is the incident power of sunlight. PCE is the most important parameter for evaluating the performance of solar cells, reflecting the ability of solar cells to do work externally. The high PCE needs to ensure that Jsc, Voc and FF all reach the highest value, which is the embodiment of the comprehensive performance

of solar cells.

## 1.2. Perovskite solar cells(PSCs)

Perovskite solar cells (PECs), mainly composed of inorganic–organic halide materials, have attracted great attention as a clean energy device, contributing to a rapid development of structure and efficiency. In the past few years, the maximum power conversion efficiencies (PCEs) have evolved from 3.8% in 2009 to 24.2% in 2019, which has been comparable with other type of solar cells. [5, 11]

### 1.2.1. Structure and characteristic of lattice

In perovskite solar cells, a three–dimensional organic–inorganic composite perovskite of the formula $ABX_3$ is mainly used, as showed in Figure 1–3, wherein A is a cation such as $MA^+(CH_3NH_3^+)$, $FA^+((NH_2)_2CH^+)$, $Cs^+$, and B is a divalent metal cation such as $Pb^{2+}$, $Sn^{2+}$ or $Ge^{2+}$, and X is a monovalent halogen anion such as $Cl^-$, $Br^-$ or $I^-$.

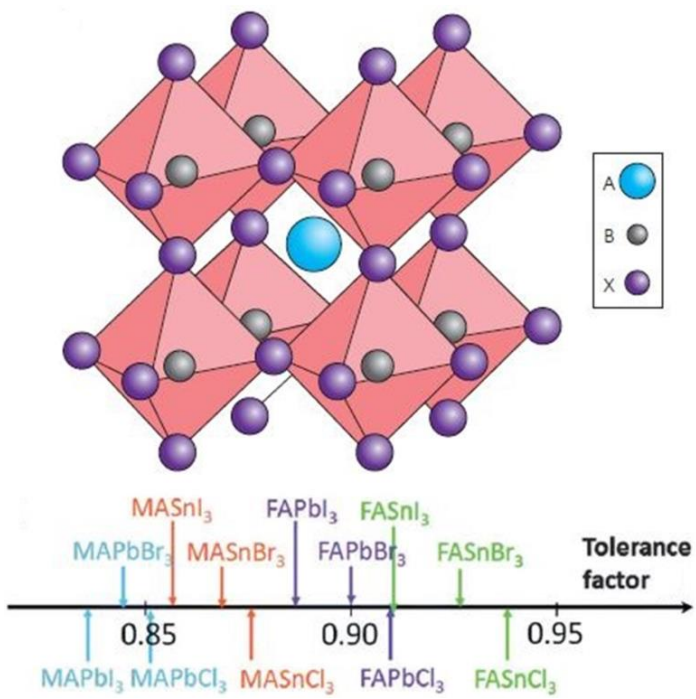


Figure 1-3 Crystal structure of perovskite [12]

Figure 1-3 is a schematic diagram of the crystal structure of a three-dimensional perovskite. In the octahedral crystal structure, the metal ion B occupies the center of the unit cell, and the halogen ion X is located at the six vertices of the octahedron with a chemical coordination bond formed with the metal ion B to stabilize the crystal lattice, and the cation A is filled between the unit cells to balance the crystal structure. [12] The allowable factor is generally used to judge whether $ABX_3$ can form a stable three-dimensional perovskite structure as

$$\tau = \frac{r_A + r_B}{\sqrt{2}\ (r_x + r_B)} \qquad (1\text{-}8)$$

Wherein $r_A$ is the radius of the cation A; $r_B$ is the radius of the metal ion B; and $r_X$ is the radius of the anion X. When the perovskite crystal lattice needs to be stable, the size of the niobium must be between 0.813 and 1.107. In Figure 1-3, perovskite material with different ion compositions is shown and it is stable for Pb and Sn perovskite. [13, 14] In addition, the octahedral factor μ ($\mu=r_B/r_X$) is between 0.44 and 0.90, which is more conducive to the stability of the cubic lattice, avoiding to the crystal phase transformation of the perovskite material by change of external condition. [12]

Inorganic-organic metal halide perovskites have many advantages as a single junction PV device such as, Suitable band gap: The conduction band and the valence band are located in the Brillouin zone at the same time, which means that perovskite has a direct band gap and can absorb photons to generate energy transition without phonon assistance. High absorption coefficient: Only 300nm's perovskite film could almost absorb all spectra of incident light, and the spectra could be adjusted for red or blue shift by introducing other kinds of ions, which bring perovskite much more useful in various ways. Excellent carrier mobility: With long carrier diffusion distance, after absorbing photons, the exitons could efficiently separate into free carriers and collected by electrode. [15, 16]

### 1.2.2. Structure of device

Depending on the configuration of the device and the direction of carrier transport, perovskite solar cells can be classified into three categories, as shown in Figure 1-4. From left to right: Mesoporous structure (MS); N-I-P plane heterojunction structure (N-I-P PHJ Structure); P-I-N plane heterojunction structure (P-I-N PHJ Structure).

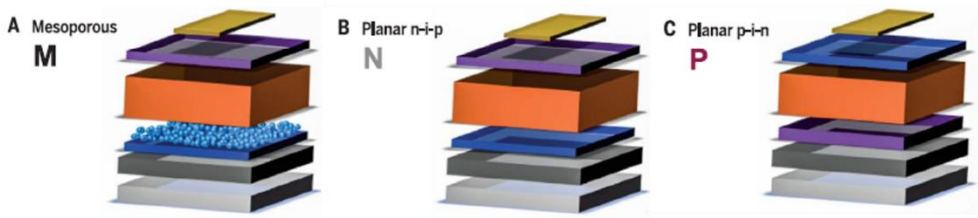


Figure 1-4 Structures of different types of PSCs [17]

1) Mesoporous structure (MS)

MS was first proposed by HJ Snaith. [18] Firstly, a layer of $TiO_2$ was prepared as an electron transport layer (ETM) on the FTO substrate, and then a metal oxide such as $TiO_2$, $Al_2O_3$, ZnO was deposited on the substrate by high-temperature sintering to form a mesoporous support layer, then the perovskite material is filled in the mesoporous layer as a light absorbing layer similar to DSSC, followed by a hole transport layer (HTM) overlying the perovskite layer and Au/Ag as an anode vapor deposited on the HTM.

2) Plane heterojunction structure (PHJ structure)

With different position of transform layer, PHJ could be divided into n-i-p PHJ and p-i-n PHJ. N-i-p has a sandwich structure with ETM(n type)/ perovskite layer/ HTM(p type) while p-i-n has a inverted structure. [14] Compared to normal structure, inverted structure is more likely to use polymer as a transport layer, which lower the preparation temperature of device and avail for flexible solar cells and other flexible electronic devices. [19-21]

### 1.2.3. Deposition method of perovskite films

The morphology of perovskite is a critical influencing factor of the performance of device, such as ability of light absorption, carrier diffusion distance, etc., so that the preparation method of perovskite films is the crux. Till now, the dominating method mainly contains one-step spin-coating, two-step dipping, interdiffusion (two-step spin-coating) and evaporation method.

One-step spin-coating method is the earliest and the most popular method. [18, 22, 23] Using a certain ratio of $PbX_2$ ($PbI_2$ , $PbBr_2$ or $PbCl_2$ ) and MAI (FAI, CsI) precursor, directly spin-coated on ETM or HTM layer, and after annealing, we could get perovskite film. The one-step method is simple to operate, however, due to the crystallization of perovskite is influenced by many factors, such as ratio of precursor solution, choose of solvent, temperature of annealing, different of atmosphere, which bring effects of the uniformity problems of film and reduce the reproducibility. [13, 14, 24]

Two-step dipping method was first proposed by M. Gräztel. After coating $PbX_2$ on the substrate, the substrate was immersed in MAI isopropanol (IPA) solution, after a while, take out the substrate and thermal annealing was done. [25] This method is also very simple especially for MS. Nevertheless, for the reaction only happens at the interface, there would be non-completed reaction and uncontrollable surface morphology. [26]

Interdiffusion method is similar with dipping method and it was first used by J. Huang. After spin-coating $PbI_2$, MAI is also coated and during the annealing process, two layers are driven to diffuse to form perovskite film. [27] Compared with dipping method, the interdiffusion method could improve the reaction probability and more controllable morphology and thickness which could be used in PHJ devices.

Evaporation method was firstly used by H.J.Snaith that two kinds of precursor materials ($PbI_2$ and MAI) in the vacuum chamber were simultaneously evaporated on the substrate. [28] This method could

form films with high uniformity and high quality. But the high production costs limit the production of large-area solar cells.

### 1.2.4. Long-term stability of PSCs

Although PSCs have a rapid development in the past ten years, the commercialization of PECs is still limited by unsolved problems about long-term stability in ambient atmosphere. [29]

The stability of PSCs is effected by many factors. When exposing in ambient air with water, UV light or other stress, the three-dimensional (3D) $ABX_3$ structure perovskite materials are prone to degrade back into precursors, which compromise the performance of PECs. Humidity acts as an aggressive cause that moisture would get into perovskite lattice and interact with perovskite, divide into MAI, $PbI_2$ and $H_2O$, seriously affects the performance of PECs. [30, 31] With encapsulation procedures, which protect the perovskite device from external sources, so that the degradation could be alleviated effectively.

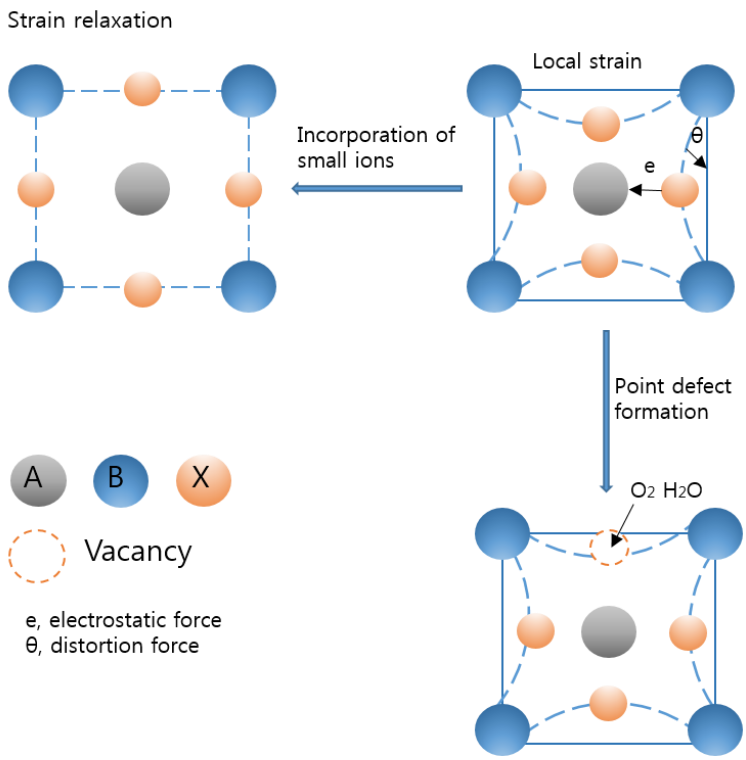


Figure 1-5 Degradation mechanism of PSCs

In addition, as the degradation mechanism showed in Figure 1-5, owing to the low formation energy of perovskite, formation of perovskite lattice always accompanies with halide vacancies, interstitial defects and substitutions. [32, 33] These defects from the surface and interiors of perovskites generally play the role of the center of non-radiative recombination effects and influent the transport rate of carriers. [34]

### 1.2.5. Stability research progress of PSCs

Lately, various treatments and methods were developed to attain better performance and stability of the perovskite devices. [35, 36] Employing functional ligands with coordination group is a way widely used for improving connection at the interface in order to get an excellent optoelectronic characteristic and moisture tolerance, where the passivation of perovskite could reduce vacancies. [37, 38] Previous research showed that when using alkyl-amines as a passivation material, due to the noncovalent hydrogen bonding interaction of alkyl-amines and under-coordinated halide anion of perovskite, it could improve crystallization and stability of perovskite film. [39] In addition, anilines were used as the passivation molecules on account of the benzene ring's hydrophobic characteristic and it effectively prevents perovskite from the outside moisture. [40]

Although there are some efficient passivation long-chain organic components, charge transporting is still limited in the modified perovskite interface. In addition, for large-size anilines molecules, which occupied much space, shows stronger steric hindrance and rigidity features in certain orientation and would also affect the ratio of decreasing defect concentration. [41, 42]

## 1.3. Purpose of research

Here we designed an innovative function material that could increase the occupied probability, namely, di-(2 picolyl) amine iodide (DMP-I) to achieve the effective interface modification of the

perovskite active layer. Relative to two picolyl ligands and an amine structure, DMP-I presents a planar configuration and carries triple iodide ions. Base on a post-treatment method, the iodide ion tends to occupy the vacancies and bond with lead ion at the interface of perovskite.[43] Compared to traditional passivation materials (here we used 3-(Aminomethyl) pyridine (AMP-I) for comparison), DMP-I has much more possibility of occupation, which has better effect of improving stability.

Relative to the reference device with the PCE of 19.69%, a champion PCE of 20.03% can be obtained. Furthermore, with the DMP-I-modified PSC shows 40% efficiency loss in dark condition (800h aging) compared to 55% efficiency loss for reference. To summarize, this novel ligand can substantially improve efficiency and stability of device. As an effective way for enhancing the performance, it is anticipated to break the bottleneck of PECs and step forward for commercialization.

# Chapter 2. Experiment

## 2.1. Materials and synthesis

### 2.1.1. Functional material synthesis

The structure of 3-(Aminomethyl) pyridine (AMP-I) and di-(2 picolyl) amine iodide (DMP-I) is showed in Figure 2-1.

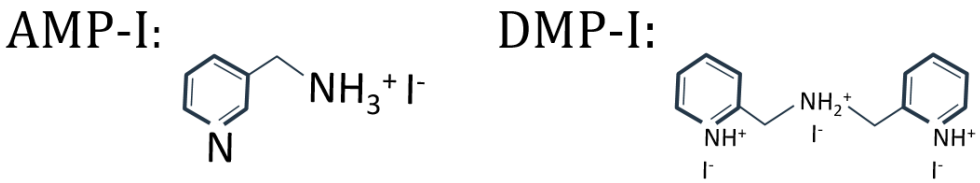


Figure 2-1 Geometry of AMP-I and DMP-I

1.99g of DMP was dissolved into 10ml methanol in flasks in ice baths, and then 70 ml HI (55% wt) aqueous solutions were added dropwise to the flasks under stirring. After reacting for 1 hour, the solutions were dried by rotary evaporator before precipitates appeared. Then the precipitates were washed by anhydrous diethyl ether for 4~5 times until the precipitates become faint yellow powders. Finally, all the powders were dried in vacuum oven at 60 ℃ overnight.

In order to confirm the structure of our synthesized material, nuclear magnetic resonance (NMR) was measured and results showed in Figure 2-2 and 2-3 prove the materials have correct geometry for both AMP-I and DMP-I. In addition, TGA in Figure 2-4 was also indicates difference between AMP-I and DMP-I.

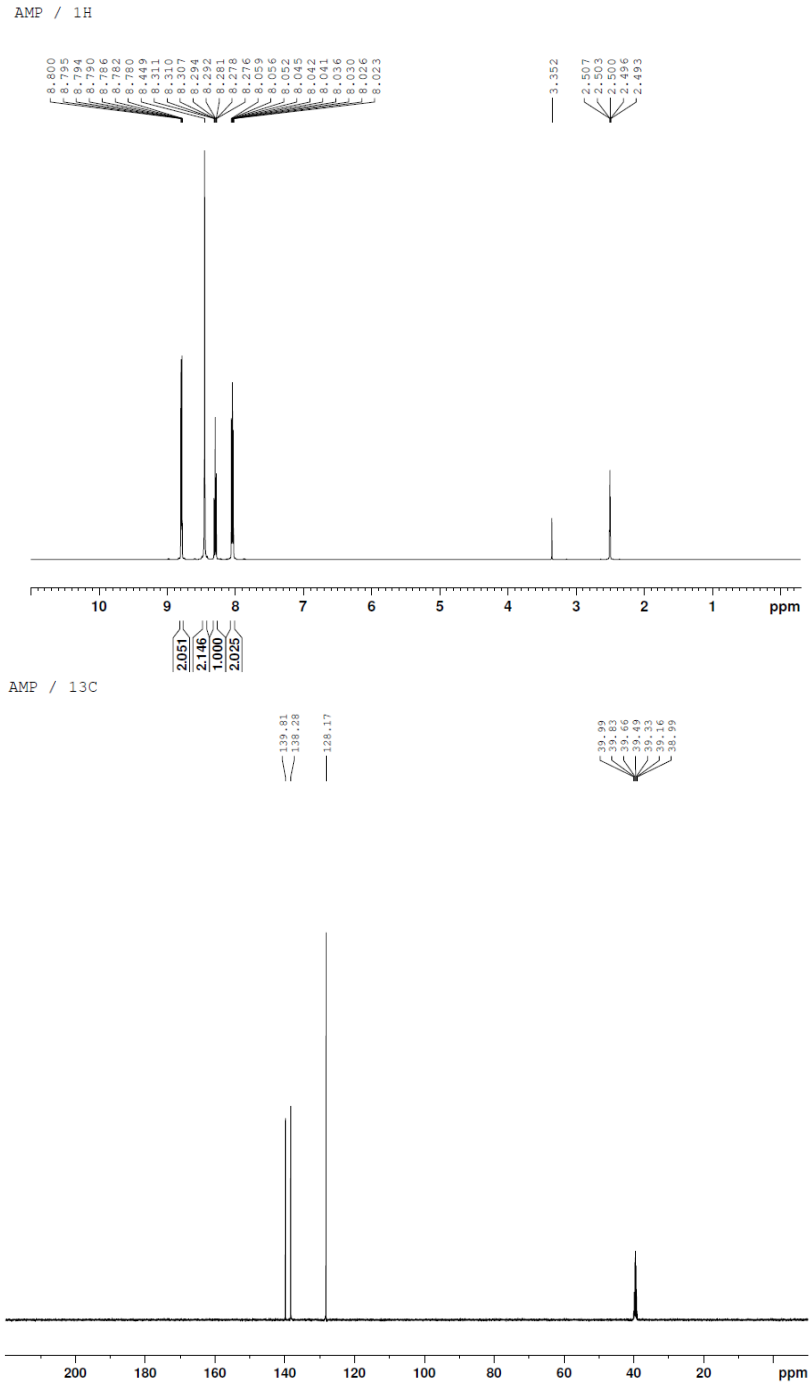


Figure 2-2 NMR result of AMP-I

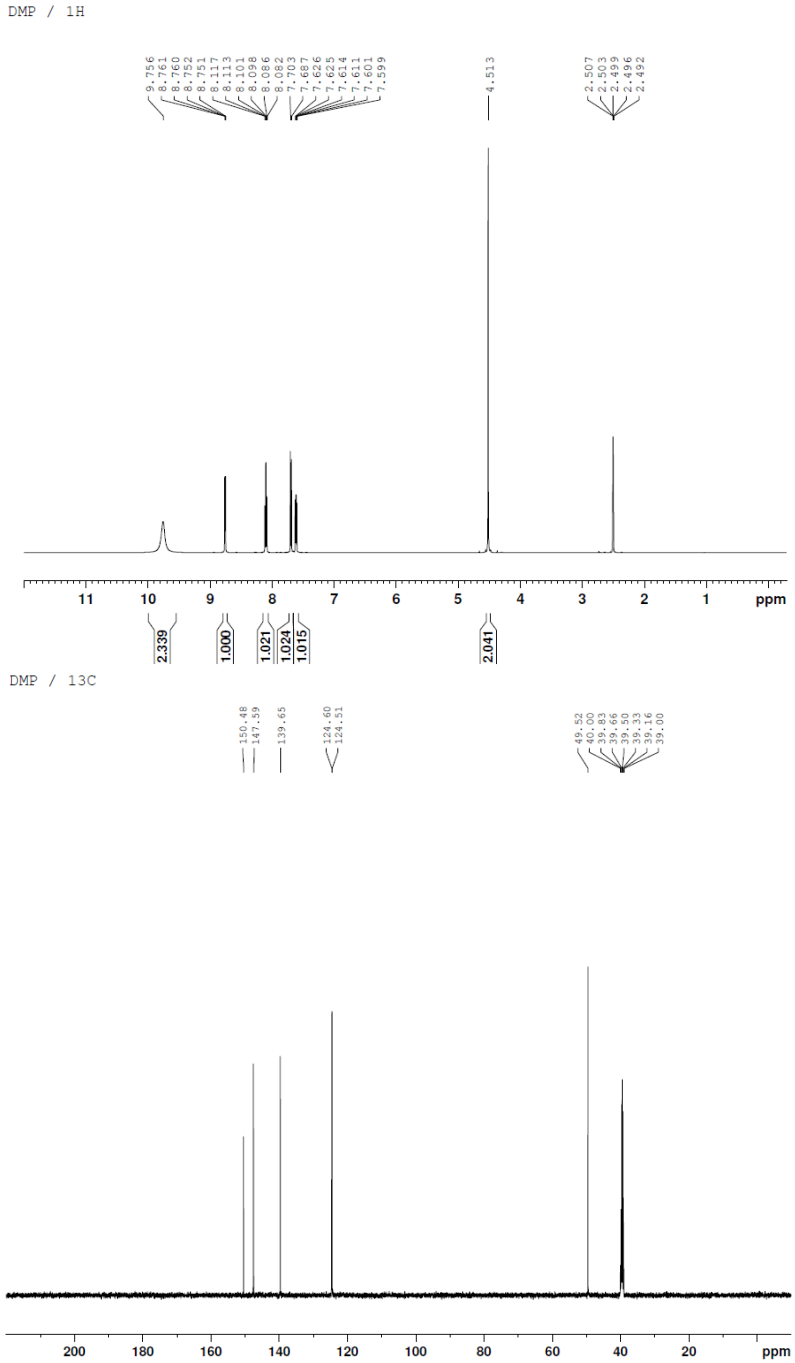


Figure 2-3 NMR result of DMP-I

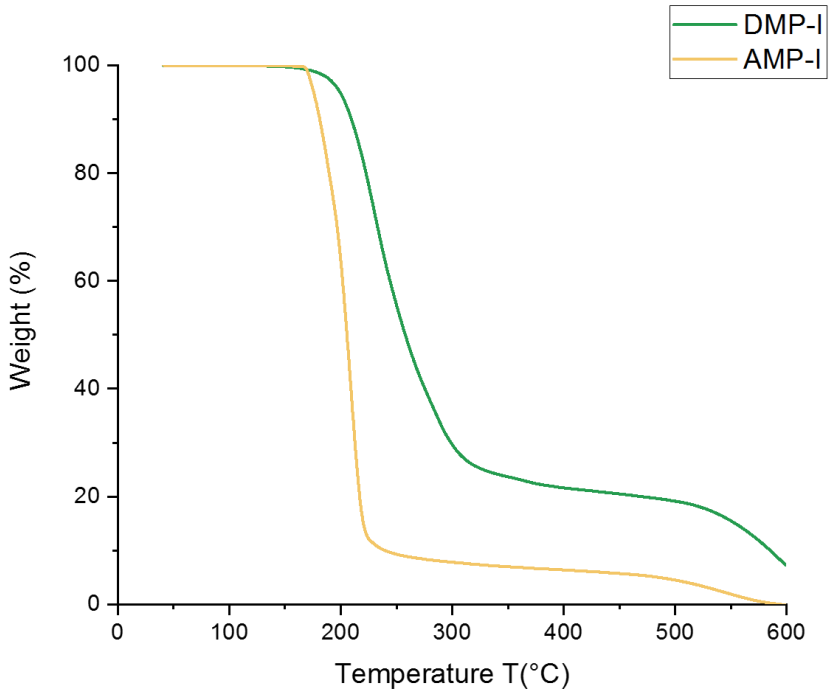


Figure 2-4 TGA result of AMP-I and DMP-I

## 2.1.2. Preparation of perovskite precursor

Our perovskite films are based on the mixed triple-cation lead mixed halide $((FAPbI_3)_{0.95}(MAPbBr_3)_{0.05})_{0.95}(CsPbI_3)_{0.05}$. (CFMPIB)

Formamidinium iodide (FAI) and methylammonium bromide (MABr) were purchased from great cell. Lead iodide ($PbI_2$), lead bromide ($PbBr_2$) and Cesium iodide (CsI) were obtained from Sigma-Aldrich. 1.3 M FA/MA/Cs perovskite material dissolved in DMF/DMSO (4:1) was made as perovskite precursor solution.

## 2.1.3. Device fabrication

The structure of PSCs device that we used (ITO/PTAA/ $((FAPbI_3)_{0.95}(MAPbBr_3)_{0.05})_{0.95}(CsPbI_3)_{0.05}$/C60/BCP/Cu) is showed in Figure 2-5 and the spin-coating fabrication sketch map of device is illustrated in Figure 2-6. ITO substrates (AMG, 9.5Ω $cm^{-2}$, 25*25 $mm^2$) were sequentially sonicated in acetone, isopropanol and deionized water. PTAA solutions (2 mg/ml in toluene) were spin

coated on ITO substrates at 6000 rpm for 40s. Then the substrates were annealed at 100 ℃ for 10 min.

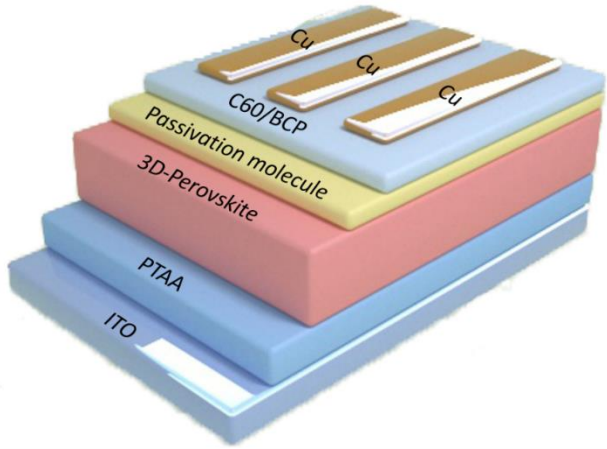


Figure 2-5 Structure of PSCs: triple perovskite with reverse structure

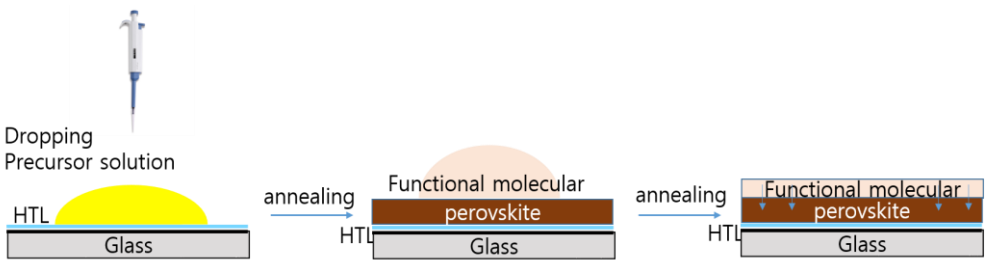


Figure 2-6 Spin-coating fabrication sketch map of perovskite solar cells

$((FAPbI_3)_{0.95}(MAPbBr_3)_{0.05})_{0.95}(CsPbI_3)_{0.05}$ film was spin-coated on top through a one-step process: the step consisting of 4000 r.p.m during 10s (preconditioning of the layer) and 20 seconds before the end of the program, 300μl of Ethyl Acetate were spin-coated on top of the perovskite layer, according to the antisolvent method previously described in literature, and finally the perovskite films were sintered at 100℃ during 30 min. [44] After that, different kinds of functional materials were spin-coated at 6000 r.p.m for 40s and annealed at 100℃ for 10 min. Then the substrates were transferred into vacuum to evaporate 20 nm C60, 6 nm bathocuproine (BCP) and 50 nm Cu at a rate of 0.2~0.3 Å/s to complete the device.

## 2.2. Characterization

### 2.2.1. Material characterization

A field emission scanning electron microscope (SEM) (AURIGA, Carl Zeiss) was used to investigate the morphologies. The XPS and UPS spectra were obtained using an Axis-Nova (Kratos) spectrometer with a He I (21.22 eV) incident radiation. XRD measurements were performed with an X-ray diffractometer (New D8 Advance, Bruker) with Cu Kα radiation. The absorption spectra were acquired using a UV-visible spectrophotometer (Cary 5000, Agilent technologies). The PL and TRPL spectra were measured by Fluoromax-4 (HORIBA) instrument.

### 2.2.2. Device characterization

J-V curves were measured by a source meter (Keithley 2400, Tektronix) under 100 mW $cm^{-2}$, AM 1.5G simulated one sun using a solar simulator (Sol 3A Class AAA 64023A, Oriel) under calibration using the KG-5 standard Si-cell (91150-KG5, Newport). Step voltage and delay time for the forward and reverse scan were set to 20 mV and 200 ms, respectively. The active area of a device was 7.29 $mm^2$ covered with a metal mask. EQE was measured by a designed EQE system with 75W Xenon lamp (USHIO, Japan).

# Chapter 3. Results and discussion

## 3.1. Film and material characteristics

To reveal the characteristic of the novel material (di-(2-picolyl) amine iodide (DMP-I)) affecting the performance of PSC, a molecule with only one picolyl ligand with similar structure, called 3-(Aminomethyl) pyridine has been used as a comparison. The morphology of the pristine film and the corresponding modified films is presented by top-view SEM image in Figure 3-1.

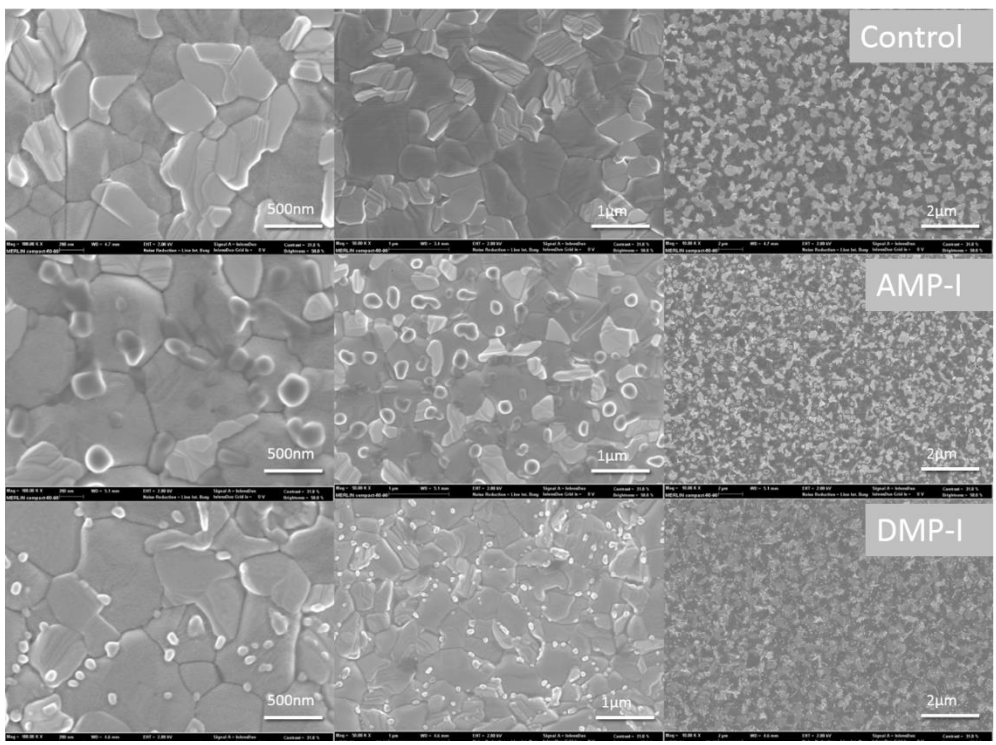


Figure 3-1 SEM images of controlled, AMP-I coated, DMP-I coated CFMPIB films, scale bar: 500nm, 1μm, 2μm, respectively

The lattice size of perovskite almost keeps the same scale with different passivating molecules, while with AMP-I some distinct spheres took shape on the top of perovskite film but with DMP-I, only small particles were formed along the grain boundaries of perovskites. In addition, the film quality of DMP-I passivation is also

better than others that less $PbI_2$ can be observed. The morphological variations in AMP-I and DMP-I were speculated that because of the different structure of two molecules, triple iodide ions could occupy more vacancies so that the formation energy of perovskite increased and make perovskite lattice more stable, as a result, less $PbI_2$ appeared on the top of perovskite. To confirm our hypothesis, the absorption spectrum and X-ray diffraction (XRD) of different perovskite films were measured.

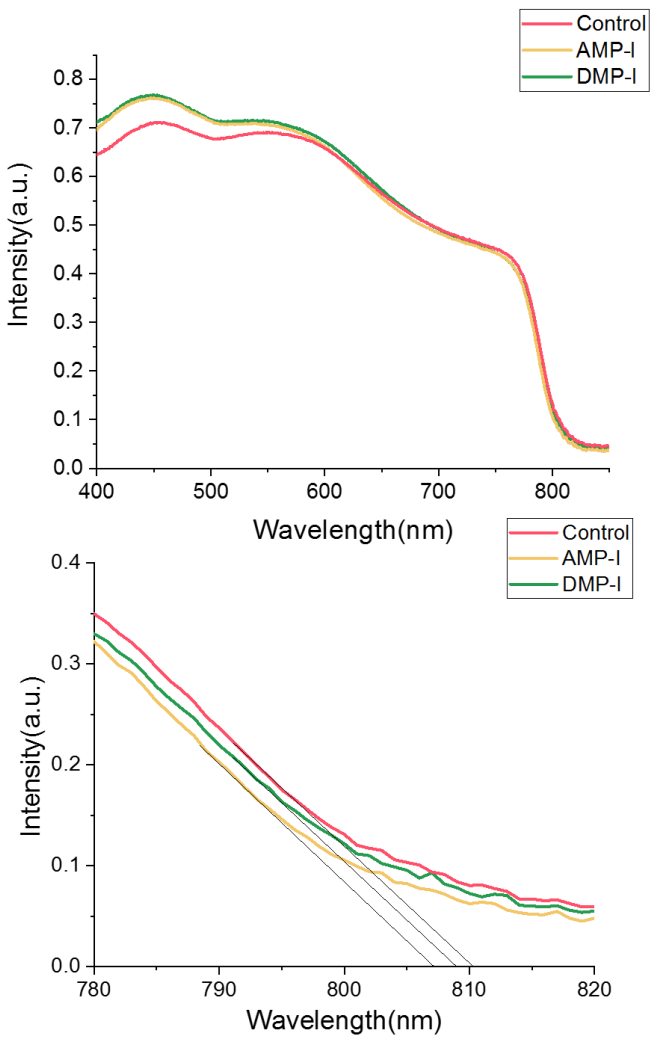


Figure 3-2 UV-visible absorption (normal, magnified)

The UV-vis absorption spectra of perovskite films are showed in Figure 3-2. From the figure we can observed that the intensity

trend of three samples almost accordant, while at short wavelength there is a slight increase of intensity when using AMP−I and DMP−I as a passivation material. This may be ascribed to some 2d structure that formed at the interface of perovskite film with a capping layer added. The absorption edge falls at around 810nm and only a slight blue shift could be observed.

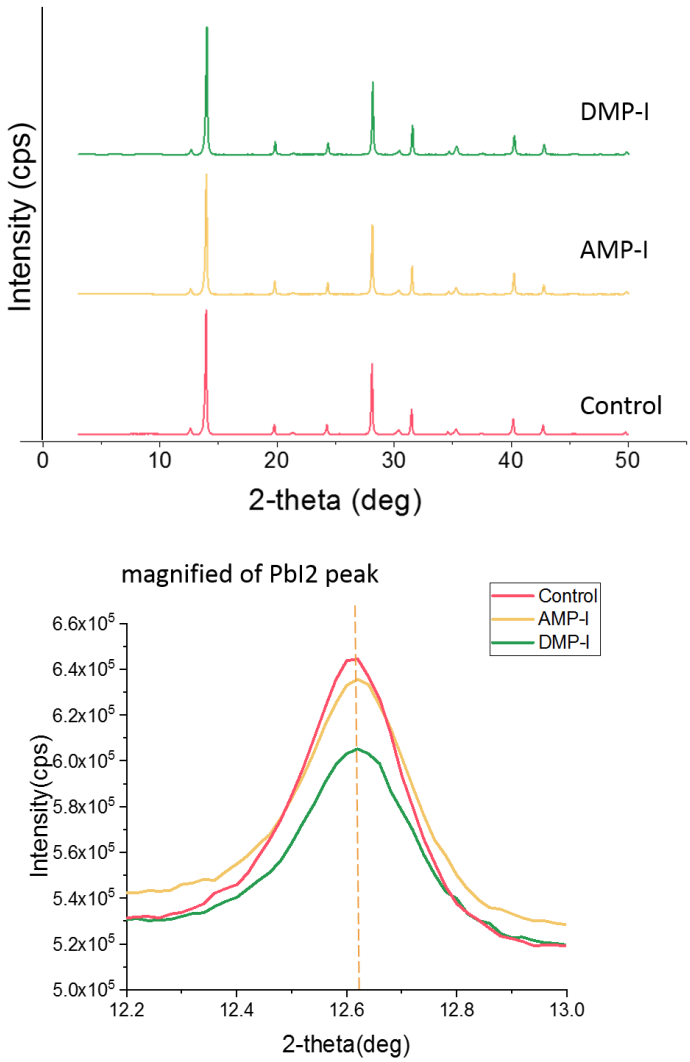


**Figure 3-3 XRD patterns of perovskite films containing different passivation molecule**

Figure 3−3 reports the XRD patterns of perovskite films containing different passivation molecule. The (110) and (220) characteristic crystal planes of CFMPIB shows two main diffraction

peaks at 14° and 28°. [45] At the same time, $PbI_2$ peak at around 12.6° was magnified in Figure 3-3 to calculate the full width at half maximum (FWHM) and as for the result, with treatment of DMP-I, narrowed FWHM and decreased intensity indicated decompose of CFMPIB had been restrain. [46] However, there were no new peaks under 10°, which means 2d perovskite structures were not formed as we speculated before.

To further understand the structure and composition evolution of CFMPIB film with passivation, X-ray photoelectron spectroscopy (XPS) and TOF-SIMS were carried out.

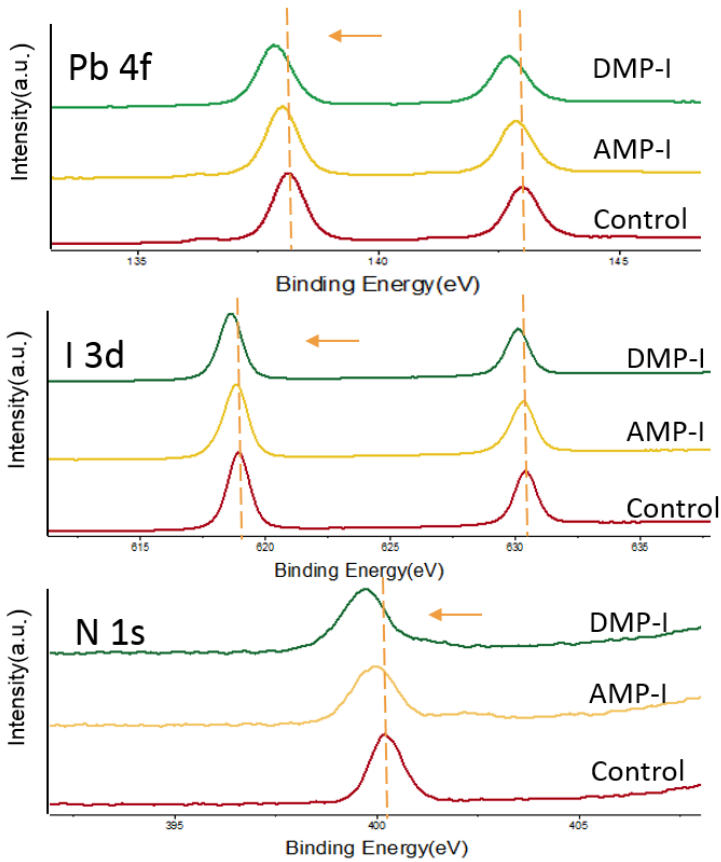


**Figure 3-4 XPS result of lead, iodide and nitrogen atoms in corresponding films**

Figure 3-4 presented the XPS results of lead, iodide and nitrogen atoms in the corresponding films. Comparing reference film, AMP-I passivation and DMP-I passivation, the lead and iodide ions'

binding energy shifted to a lower level on account of bond angle of two ions increased when functional molecule added. In addition, we could observe that intensity of $Pb_0$ gets smaller in sequence which showed the possibility of lead ions being oxidized decreased and it agrees with our former analysis. N atom with two different peaks in AMP-I and DMP-I post-treated films could be observed in the result, which contains two different binding energy and showed the existence of molecule that used for passivation.

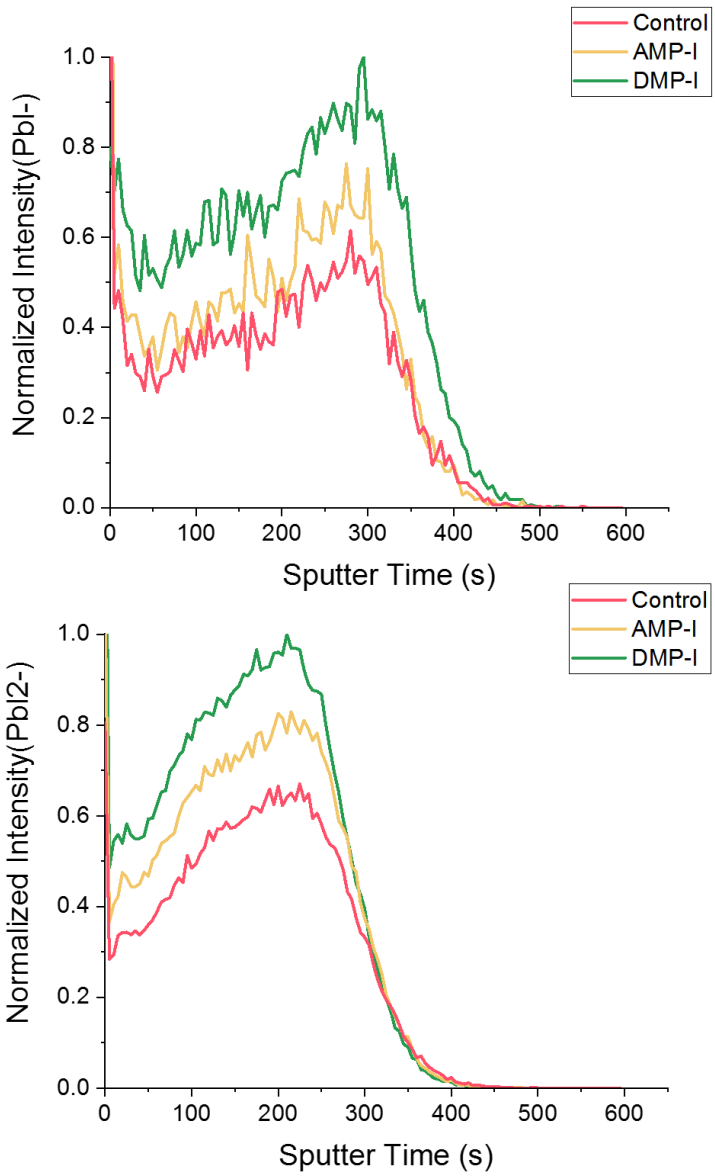


Figure 3-5 TOM-SIMs of different ions in controlled, AMP-I and DMP-I films

Similarly, the results of TOF-SIMS (Figure 3-5) also showed higher intensity of $PbI^-$ ion that the combination of lead and iodide has been increased by passivation. With the thin functional layer formed on the surface of the original film, defects in perovskite layer are much more occupied by AMP-I material and a distinct increase could be noticed by adding DMP-I material.

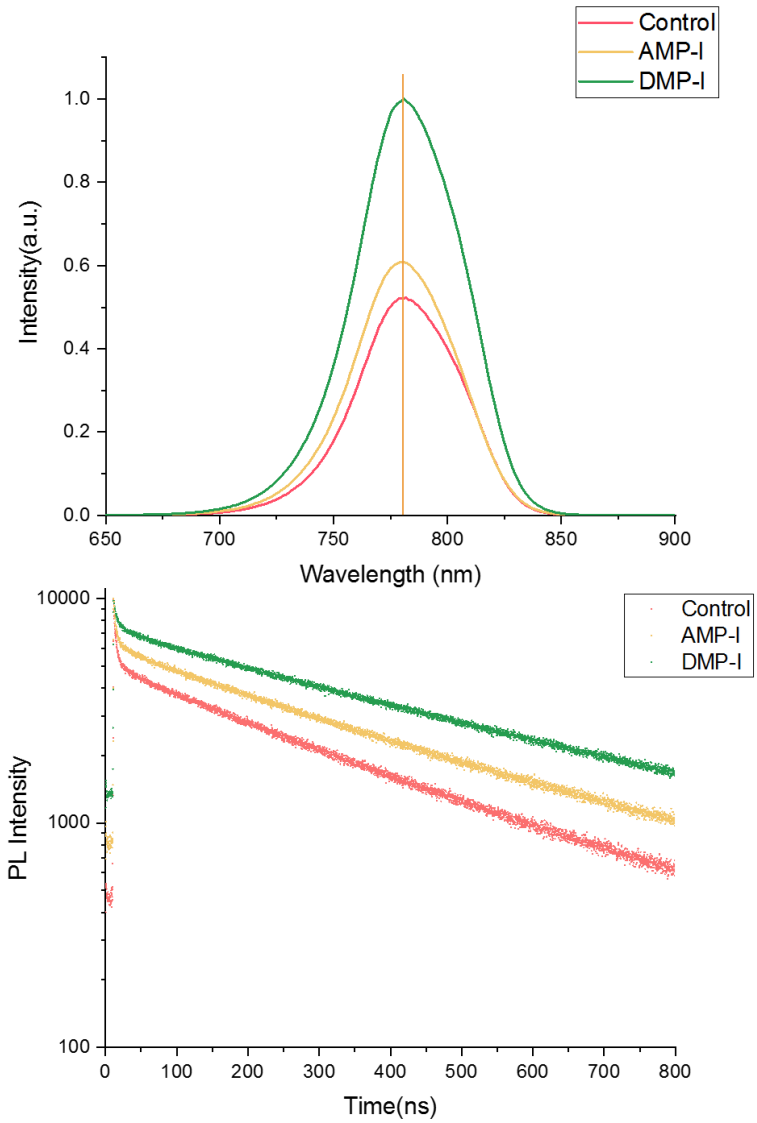


Figure 3-6 PL and TRPL of typical corresponding films

Steady-state photoluminescence (PL) spectra and time-

resolved photo luminescence (TRPL) of corresponding films are exhibited in Figure 3-6. For PL, we can observe that after introducing passivation molecules (AMP-I and DMP-I) into perovskite film, the peak of steady-state increased and a PL peak blue-shifted slightly. The increased intensity of PL could attribute to enhanced charge carrier radiative recombination by passivated with the functional molecules. [47] In addition, the more efficient band-to-band direct recombination would contribute a blue shift effect here. As for TRPL, carrier lifetime is progressively raised from 348ns to 575ns with DMP-I added, revealing more decent carrier transport. The growth of carrier lifetime can be ascribed to the increasing exciton radiative recombination and less non-radiative recombination for DMP-I occupied more vacancies at the interface of perovskite layer and helped the carrier transportation between lattices.

Based on the analysis of morphology variation, XRD, XPS, TRPL and other measurements, the post-treatment of using DMP-I as a passivation molecule could achieve a modification process on perovskite films. With AMP-I, although there is some improvement on film and lattice characteristic, decompose of CFMPIB is a fatal shortcoming when using as a functional material for stability. On the contrary, DMP-I with superiority of structure, may be an ideal molecule to improve the performance of PECs.

## 3.2. J-V characteristics

Above all, film and material characteristics have been discussed and to evaluate the effect of DMP-I passivation, planar inverted heterojunction structure devices with different passivation materials were fabricated. The device that we used was composed of ITO/ PTAA/$((FAPbI_3)_{0.95}(MAPbBr_3)_{0.05})_{0.95}(CsPbI_3)_{0.05}$/C60/BCP/Cu, structure of device is showed in Figure 2-5 with the fabricate method mentioned above.

### 3.2.1. Photovoltaic parameters

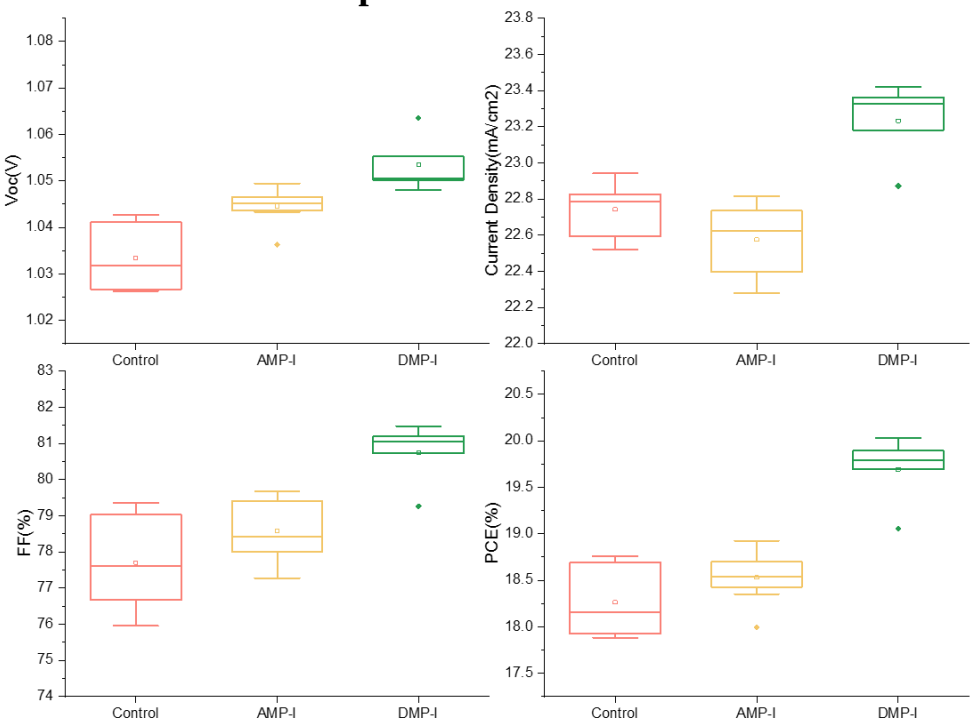


Figure 3-7 Statistical distributions of device photovoltaic parameters of corresponding PECs

We fabricated more than 100 PSCs for different passivation molecules, the PCEs are summarized in Figure 3-7. The champion device is showed in Figure 3-8 with DMP-I film exhibited that open-circuit voltage (Voc) of 1.06 V, short-circuit current (Jsc) of 23.42 mA $cm^{-2}$, with a fill factor (FF) of 81.47%, we finally got a 20.03% of PCE. Also, we tested the corresponding incident photon conversion efficiency (IPCE) of PSC (Figure 3-8). We could observe that Voc and FF got an increase due to the post-treatment and DMP-I showed better performance, while for Jsc of AMP-I, a decrease can be speculated due to a perishing connection at the interface of perovskite. Base on the increasing parameters, DMP-I post-treatment can slightly increase the PCE of PECs.

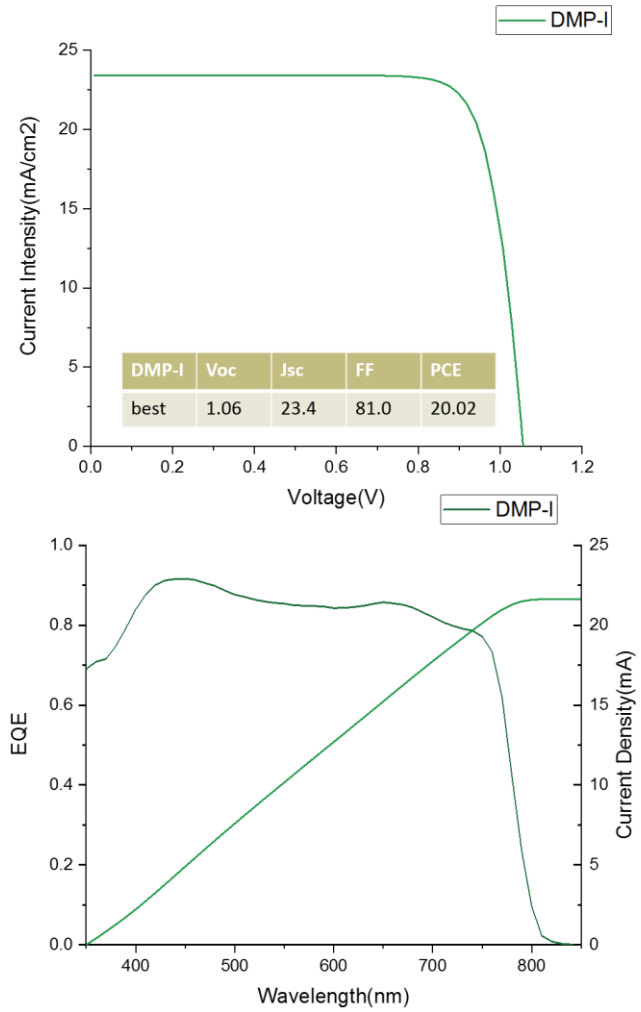


Figure 3-8 J-V curve and IPCE of the champion DMP-I treated device

## 3.2.2. Long-term stability

To study the stability effect of the passivation layer, we examined the long-term stability of corresponding devices under dark storage in ambient atmosphere and showed the results in Figure 3-9. Compare to the reference device and device with AMP-I, DMP-I had a remarkable improvement, retaining 60% of the initial PCE after 800 hours. The stability test shows a significant effect for DMP-I used as a passivation molecule that enhances the stability and performance for PSCs.

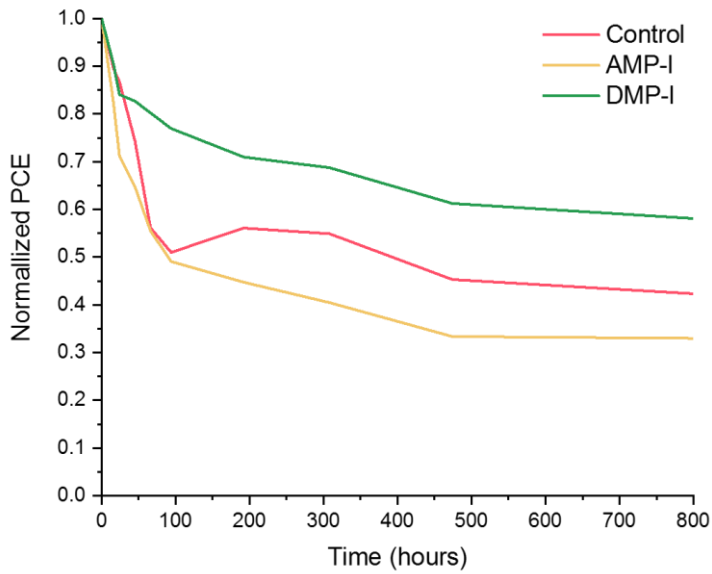


Figure 3-9 Normalized PCE dependent on time of unencapsulated controlled and passivated device stored in ambient air

# Chapter 4. Conclusion and future work

In conclusion, here we designed innovative functional molecule to post-engineer interfaces of perovskite leads to improve both stability and efficiency of perovskite solar cells. By analyzing the characteristics of the material and film, the charge extraction and transport could be significantly enhanced due to the effective occupation of vacancies in perovskite film. Furthermore, the occupation also prevents perovskite from degradation and reaction with moisture and oxygen from the outside environment. Thanks to above-mentioned advantages of this novel molecule, over 20% efficiency of the best solar cell with a better long-term stability (maintaining 60% of performance after 800h testing, 25℃, and 40±10 humidity).

We hope this effective approach could inspire research of designed passivation materials, which could further promote the stability and performance of PSCs. In addition, combined with encapsulation process, the stability of PSCs could move forward a step and accelerate the commercialization of PSCs in the future.

# Bibliography


[1] P. V. Kamat, "Meeting the clean energy demand: nanostructure architectures for solar energy conversion," *The Journal of Physical Chemistry C,* vol. 111, no. 7, pp. 2834-2860, 2007.

[2] K. Barnham, M. Mazzer, and B. Clive, "Resolving the energy crisis: nuclear or photovoltaics?," *Nature materials,* vol. 5, no. 3, p. 161, 2006.

[3] G. J. Meyer, "Molecular approaches to solar energy conversion with coordination compounds anchored to semiconductor surfaces," *Inorganic chemistry,* vol. 44, no. 20, pp. 6852-6864, 2005.

[4] D. M. Chapin, C. Fuller, and G. Pearson, "A new silicon p-n junction photocell for converting solar radiation into electrical power," *Journal of Applied Physics,* vol. 25, no. 5, pp. 676-677, 1954.

[5] NREL, "Best Research-Cell Efficiency Chart," 2019.

[6] M. A. Green *et al.*, "Solar cell efficiency tables (version 50)," *Progress in Photovoltaics: Research and Applications,* vol. 25, no. 7, pp. 668-676, 2017.

[7] A. Hagfeldt, G. Boschloo, L. Sun, L. Kloo, and H. Pettersson, "Dye-sensitized solar cells," *Chemical reviews,* vol. 110, no. 11, pp. 6595-6663, 2010.

[8] S. Günes, H. Neugebauer, and N. S. Sariciftci, "Conjugated polymer-based organic solar cells," *Chemical reviews,* vol. 107, no. 4, pp. 1324-1338, 2007.

[9] A. Nozik, "Quantum dot solar cells," *Physica E: Low-dimensional Systems and Nanostructures,* vol. 14, no. 1-2, pp. 115-120, 2002.

[10] M. A. Green and S. P. Bremner, "Energy conversion approaches and materials for high-efficiency photovoltaics," *Nature materials,* vol. 16, no. 1, p. 23, 2017.

[11] A. Kojima, K. Teshima, Y. Shirai, and T. J. J. o. t. A. C. S. Miyasaka, "Organometal halide perovskites as visible-light sensitizers for photovoltaic cells," *Journal of the American Chemical Society,* vol. 131, no. 17, pp. 6050-6051, 2009.

[12] M. A. Green, A. Ho-Baillie, and H. J. Snaith, "The emergence of perovskite solar cells," *Nature Photonics,* vol. 8, no. 7, pp. 506-514, 2014.

[13] H.-S. Kim, S. H. Im, and N.-G. Park, "Organolead Halide Perovskite: New Horizons in Solar Cell Research," *Journal of Physical Chemistry C,* vol. 118, no. 11, pp. 5615–5625, 2014.

[14] Y. Zhao and K. Zhu, "Organic–inorganic hybrid lead halide perovskites for optoelectronic and electronic applications," *Chemical Society Reviews,* vol. 47, no. 13, pp. 655-689, 2016.

[15] S. D. Stranks *et al.*, "Electron-hole diffusion lengths exceeding 1 micrometer in an organometal trihalide perovskite absorber," *Science,* vol. 342, no. 6156, pp. 341-344, 2013.

[16] Y. Shi *et al.*, "A Strategy for Architecture Design of Crystalline Perovskite Light-Emitting Diodes with High Performance," *Advanced*

*Materials,* vol. 30, no. 25, p. 1800251, 2018.
[17] J.-P. Correa-Baena *et al.*, "Promises and challenges of perovskite solar cells," *Science,* vol. 358, no. 6364, pp. 739-744, 2017.
[18] M. M. Lee, J. Teuscher, T. Miyasaka, T. N. Murakami, and H. J. Snaith, "Efficient Hybrid Solar Cells Based on Meso-Superstructured Organometal Halide Perovskites," *Science,* vol. 338, no. 6107, pp. 643-647, 2012.
[19] Q. Lin, A. Armin, R. C. R. Nagiri, P. L. Burn, and P. Meredith, "Electro-optics of perovskite solar cells," *Nature Photonics,* vol. 9, no. 2, pp. 106-112, 2015.
[20] H. Azimi *et al.*, "A Universal Interface Layer Based on an Amine-Functionalized Fullerene Derivative with Dual Functionality for Efficient Solution Processed Organic and Perovskite Solar Cells," *Advanced Energy Materials,* vol. 5, no. 8, pp. 767-72, 2015.
[21] Z. Bin, J. Li, L. Wang, and D. Lian, "Efficient n-type dopants with extremely low doping ratios for high performance inverted perovskite solar cells," *Energy & Environmental Science,* vol. 9, no. 11, 2016.
[22] H. Zhou *et al.*, "Interface engineering of highly efficient perovskite solar cells," *Science,* vol. 345, no. 6196, pp. 542-546, 2014.
[23] N. J. Jeon, J. H. Noh, Y. C. Kim, W. S. Yang, S. Ryu, and S. I. Seok, "Solvent engineering for high-performance inorganic–organic hybrid perovskite solar cells," *Nature Materials,* vol. 13, no. 9, pp. 897-903, 2014.
[24] H. Kim, K. G. Lim, and T. W. Lee, "Planar heterojunction organometal halide perovskite solar cells: Roles of interfacial layers," *Energy & Environmental Science,* vol. 9, no. 1, pp. 12-30, 2016.
[25] J. Burschka *et al.*, "Sequential deposition as a route to high-performance perovskite-sensitized solar cells," *Nature,* vol. 499, no. 7458, pp. 316-319, 2013.
[26] P. Docampo and T. Bein, "A Long-Term View on Perovskite Optoelectronics," *Acc Chem Res,* vol. 49, no. 2, pp. 339-346, 2016.
[27] Z. Xiao *et al.*, "Efficient, high yield perovskite photovoltaic devices grown by interdiffusion of solution-processed precursor stacking layers," *Energy & Environmental Science,* vol. 7, no. 8, pp. 2619-2623, 2014.
[28] M. Liu, M. B. Johnston, and H. J. Snaith, "Efficient planar heterojunction perovskite solar cells by vapour deposition," *Nature,* vol. 501, no. 7467, p. 395, 2013.
[29] J. Chen, J. Y. Seo, and N. G. Park, "Simultaneous improvement of photovoltaic performance and stability by in situ formation of 2D perovskite at (FAPbI3) 0.88 (CsPbBr3) 0.12/CuSCN interface," *Advanced Energy Materials,* vol. 8, no. 12, p. 1702714, 2018.
[30] J.-P. Correa-Baena *et al.*, "The rapid evolution of highly efficient perovskite solar cells," *Energy & Environmental Science,* vol. 10, no. 3, pp. 710-727, 2017.
[31] N. Ahn *et al.*, "Trapped charge-driven degradation of perovskite solar cells," *Nature communications,* vol. 7, p. 13422, 2016.
[32] L. N. Quan *et al.*, "Ligand-stabilized reduced-dimensionality

perovskites," *Journal of the American Chemical Society,* vol. 138, no. 8, pp. 2649-2655, 2016.
[33] W.-J. Yin, T. Shi, and Y. J. A. P. L. Yan, "Unusual defect physics in CH3NH3PbI3 perovskite solar cell absorber," *Applied Physics Letters,* vol. 104, no. 6, p. 063903, 2014.
[34] M. Yang *et al.*, "Do grain boundaries dominate non-radiative recombination in CH 3 NH 3 PbI 3 perovskite thin films?," *Physical Chemistry Chemical Physics,* vol. 19, no. 7, pp. 5043-5050, 2017.
[35] Y. Bai, X. Meng, and S. J. A. E. M. Yang, "Interface engineering for highly efficient and stable planar p-i-n perovskite solar cells," *Advanced Energy Materials,* vol. 8, no. 5, 2018.
[36] H. J. J. N. m. Snaith, "Present status and future prospects of perovskite photovoltaics," *Nature materials,* vol. 17, no. 5, p. 372, 2018.
[37] K. T. Cho *et al.*, "Water-repellent low-dimensional fluorous perovskite as interfacial coating for 20% efficient solar cells," *Nano letters,* vol. 18, no. 9, pp. 5467-5474, 2018.
[38] H. Dong *et al.*, "Conjugated Molecules "Bridge": Functional Ligand toward Highly Efficient and Long-Term Stable Perovskite Solar Cell," *Advanced Functional Materials* p. 1808119, 2019.
[39] T. Zhao, C.-C. Chueh, Q. Chen, A. Rajagopal, and A. K.-Y. J. A. E. L. Jen, "Defect passivation of organic–inorganic hybrid perovskites by diammonium iodide toward high-performance photovoltaic devices," *ACS Energy Letters,* vol. 1, no. 4, pp. 757-763, 2016.
[40] A. Fakharuddin, L. Schmidt-Mende, G. Garcia-Belmonte, R. Jose, and I. J. A. E. M. Mora-Sero, "Interfaces in perovskite solar cells," *Advanced Energy Materials,* vol. 7, no. 22, p. 1700623, 2017.
[41] W.-H. Lee *et al.*, "Boosting thin-film perovskite solar cell efficiency through vacuum-deposited sub-nanometer small-molecule electron interfacial layers," *Nano Energy* vol. 38, pp. 66-71, 2017.
[42] Y. Lin *et al.*, "π-Conjugated Lewis Base: Efficient Trap-Passivation and Charge-Extraction for Hybrid Perovskite Solar Cells," *Advanced materials,* vol. 29, no. 7, p. 1604545, 2017.
[43] L. Mao *et al.*, "Hybrid Dion–Jacobson 2D lead iodide perovskites," *Journal of the American Chemical Society,* vol. 140, no. 10, pp. 3775-3783, 2018.
[44] N. Ahn, D.-Y. Son, I.-H. Jang, S. M. Kang, M. Choi, and N.-G. Park, "Highly reproducible perovskite solar cells with average efficiency of 18.3% and best efficiency of 19.7% fabricated via Lewis base adduct of lead (II) iodide," *Journal of the American Chemical Society,* vol. 137, no. 27, pp. 8696-8699, 2015.
[45] H. S. Kim, J. Y. Seo, and N. G. J. C. Park, "Material and device stability in perovskite solar cells," *ChemSusChem,* vol. 9, no. 18, pp. 2528-2540, 2016.
[46] Z. Wang, Q. Lin, F. P. Chmiel, N. Sakai, L. M. Herz, and H. J. J. N. E. Snaith, "Efficient ambient-air-stable solar cells with 2D–3D heterostructured butylammonium-caesium-formamidinium lead halide perovskites," *Nature Energy,* vol. 2, no. 9, p. 17135, 2017.
[47] M. B. Johnston and L. M. Herz, "Hybrid Perovskites for Photovoltaics:

Charge-Carrier Recombination, Diffusion, and Radiative Efficiencies," *Acc Chem Res,* vol. 49, no. 1, pp. 146-154, 2016.

# Acknowledgement

Firstly, I would like to give thanks to my advisor: Prof. Mansoo, Choi. Thanks to his help and encouragements and the nice research environment that he provide that I could successfully finish my master degree.

Secondly, I love to say thank you to Dr. Jun Xi, who gave a lot of help about my research and his passion of doing research also inspired me a lot in these years. In addition, thanks to other members in our lab, who always helped me on doing experiment and encouraged me when I was down.

Next, thanks to Overseas Koreans Foundation funded me during my master course and provided a good platform for me to connect with other overseas Koreans.

Finally, thanks to my parents and other friends not be mentioned here. Thanks for staying by my side and supporting me all the time.